Time dependence of liquid-helium fluorescence

D. N. McKinsey,[1,*] C. R. Brome,[1] S. N. Dzhosyuk,[1] R. Golub,[2] K. Habicht,[2] P. R. Huffman,[3] E. Korobkina,[2] S. K. Lamoreaux,[4] C. E. H. Mattoni,[1] A. K. Thompson,[3] L. Yang,[1] and J. M. Doyle[1]

[1]*Department of Physics, Harvard University, Cambridge, Massachusetts 02138, USA*

[2]*Hahn-Meitner Institut, Berlin-Wannsee, Germany*

[3]*National Institute of Standards and Technology, Gaithersburg, Maryland 20899, USA*

[4]*Los Alamos National Laboratory, Los Alamos, New Mexico 87544, USA*

(Received 7 January 2003; published 26 June 2003)

The time dependence of extreme ultraviolet (EUV) fluorescence following an ionizing radiation event in liquid helium is observed and studied in the temperature range from 250 mK to 1.8 K. The fluorescence exhibits significant structure including a short ($\sim$10 ns) strong initial pulse followed by single photons whose emission rate decays exponentially with a 1.6-μs time constant. At an even longer time scale, the emission rate varies as ''1/time'' (inversely proportional to the time after the initial pulse). The intensity of the ''1/time'' component from β particles is significantly weaker than those from α particles or neutron capture on ^{3}He. It is also found that for α particles, the intensity of this component depends on the temperature of the superfluid helium. Proposed models describing the observed fluorescence are discussed.

DOI: 10.1103/PhysRevA.67.062716 PACS number(s): 34.50.Gb, 33.50.−j, 82.20.Pm

I. INTRODUCTION

Liquid-helium scintillation was discovered in 1959 by Thorndike and Shlaer [1] and by Fleishman, Einbinder, and Wu [2]. The scintillation light was found not to pass through any standard window materials, even ones with very low cutoff wavelengths such as LiF [3]. However, by coating the inside of the glass vessel used to contain the helium with an organic fluor, the light was ''converted'' to the visible and detected with a photomultiplier tube. Through these initial experiments and others, it was confirmed that the helium scintillation light was primarily in the extreme ultraviolet (EUV) spectral region.

Studying the scintillation pulses more carefully, Moss and Hereford found that the scintillation intensity from α sources had a peculiar temperature dependence below the λ point [4]. Kane *et al*. then showed that β sources did not display the same behavior [5]. Based on this observation, Hereford and Moss speculated that collisions of the excited scintillation species played a role and the scintillation could come from excited atoms or metastable states of the liquid [6]. Later, Jortner *et al*. showed that if impurities were suspended in the helium, they fluoresced in the visible, suggesting energy transfer from a helium metastable state to the impurity [7].

During this pioneering work on scintillation, liquid helium was also under intense investigation for its fascinating superfluid properties. Its low-energy excitations (phonons, rotons, and vortices) were a rich source of information about the superfluid state, and were the subject of much experimentation. In 1968, Surko and Reif discovered a new, fourth kind of long-lived neutral excitation [8]. By immersing an α source (^{210}Po) in cold ($T<0.6$ K) superfluid helium, excitations were produced that could travel through the liquid for distances greater than 1 cm without appreciable scattering or attenuation. These could cause He^+ ions and electrons to be emitted from the surface of the liquid helium, or positive ions and electrons to be emitted from a metal plate placed in the liquid. Because the excitations were of sufficient energy to ionize helium atoms ($E_i=24.6$ eV), they clearly were much more energetic than phonons, rotons, and vortices; however, the nature of these new neutral excitations was unknown. Later work showed that there was a substantial delay between the creation of the excitations and their arrival at the surface, and that they could also be produced by β excitation [9,10].

An experiment then gave reason to believe that the source of the EUV scintillation light and the unknown neutral excitation were both excited helium electronic states. In 1969, Dennis *et al*. measured the visible and near-infrared light spectrum from liquid helium bombarded by an intense, 160-keV electron beam and found emission from both helium atoms and diatomic helium molecules [11]. In particular, it was shown that the molecular singlet and triplet ground states, $He_2(A^1\Sigma_u^+)$ and $He_2(a^3\Sigma_u^+)$, were populated. Both of these molecules are unstable for radiative decay to two ground-state helium atoms and both emit a 16 eV (80 nm) photon when they decay. However, the radiative lifetimes of the two states in vacuum (and it turns out in liquid He) are much different. The $He_2(A^1\Sigma_u^+)$ molecule decays in about 1 ns [12], whereas the radiative lifetime of the $He_2(a^3\Sigma_u^+)$ molecule in liquid helium is on the order of 10 s, since the decay to two helium atoms requires an electron-spin flip [13,14]. The $He_2(a^3\Sigma_u^+)$ molecule was thus a plausible candidate for the neutral excitation discovered by Surko and Reif [8], while $He_2(A^1\Sigma_u^+)$ was the source of scintillation pulses.

Additional experiments were performed by measuring the transient behavior of individual atomic and molecular emission bands emanating from the liquid. If the electron beam

*Corresponding author. Present address: Department of Physics, Princeton University, Princeton, NJ 08544. Email address: mckinsey@princeton.edu

was suddenly turned off at time $t=0$, then the density of $He_2(a^3\Sigma_u^+)$ molecules was seen to decay rapidly, with a t^{-1} dependence [15–17]. This behavior could be explained by the hypothesis that $He_2(a^3\Sigma_u^+)$ molecules react with each other by Penning ionization:

$$He_2 + He_2 \rightarrow 3He + He^+ + e^-$$

or

$$He_2 + He_2 \rightarrow 2He + {He_2}^+ + e^-.$$

Penning ionization can occur because the two excited helium molecules together have enough internal energy to ionize a helium atom. It requires no activation energy and occurs with nearly unity probability if the molecules collide. Penning ionization is a two-body reaction; this implies that the concentration M of metastable molecules is described by the equation $dM/dt=-\alpha M^2$, which has the solution $M=M_0/(1+M_0\alpha t)$, where α is the bilinear reaction coefficient and M_0 is the initial concentration of $He_2(a^3\Sigma_u^+)$ molecules. The reaction coefficient α was measured to be about 10^{-9} cm^3 s^{-1} at 1.4 K [16], and found to decrease with increasing temperature, indicating that the reaction rate is affected by the roton density in the liquid. The higher the temperature, the higher the roton density, and the longer it takes for two molecules to diffuse through the roton gas, find each other, and react.

It was also found that metastable $He(2^3S)$ atoms are created in copious numbers by an electron beam passing through the liquid-helium. But though this atom has an 8000 s radiative lifetime in vacuum [18], it does not last long in the helium liquid. The $He(2^3S)$ density was found to drop exponentially, with a 15 μs lifetime. A concurrent rise in density of vibrationally excited $He_2(a^3\Sigma_u^+)$ molecules was also seen, lending evidence to the hypothesis that in the dense liquid-helium environment, ground-state helium atoms can tunnel into the (2^3S) potential, forming vibrationally excited $He_2(a^3\Sigma_u^+)$ molecules. This reaction does not happen instantaneously because there is a 60-meV potential barrier between the $He(2^3S)$ and $He(1^1S)$ atoms [19]. At high helium densities, multibody effects can lower the barrier significantly.

Further work on the helium scintillation system included measuring the extreme ultraviolet scintillation spectrum using a grating EUV spectrometer [20–22]. It was found that a very intense continuum was produced in the wavelength range from 60 nm to 100 nm, corresponding to the reaction

$$He_2(A^1\Sigma_u^+) \rightarrow 2He(1^1S) + h\nu.$$

The EUV spectrum is centered at 80 nm [22], and exhibits a large wavelength spread, a consequence of the fact that the reaction product (two free helium atoms) is not a bound state. In the Oppenheimer approximation, the slowly moving helium nuclei do not change position during a fast electronic transition. Therefore, the amount of energy released as light depends on the distance between the two He nuclei at the time of radiative decay. The remaining energy goes into kinetic energy of the two final 1^1S helium atoms.

It was also found that varying the location of the electron beam relative to the liquid-helium surface had little effect on the measured EUV intensity. The scintillation light was unattenuated by as much as 10 cm of liquid helium. The transparency of liquid helium to its own scintillation light can be explained by the high energy needed to excite atomic helium: the difference in energy between the 1^1S ground state and the first atomic helium excited state is 20 eV, more energy than the 16 eV photons emitted in helium excimer decay. The fact that singlet production is enhanced in the liquid, plus the fact that helium does not absorb its own scintillation light, results in an extremely bright EUV pulse from $He_2(A^1\Sigma_u^+)$ decay. In fact, the ultraviolet emission accounts for over 99% of the total scintillation intensity [20]. The extraordinary intensity of the ultraviolet emission has been measured recently by Adams *et al.*; they find that 35% of the energy deposited by β particles in superfluid helium is emitted as prompt EUV light [23,24].

Because the $He_2(a^3\Sigma_u^+)$ molecules are destroyed by the Penning ionization in experiments that require high excitation densities, the spectra in these experiments are dominated by $He_2(A^1\Sigma_u^+)$, which can radiatively decay before reacting with other metastables [16,17]. Recent experiments [25] showed no suppression of the Penning ionization in magnetic fields up to 5.5 T. But while triplet molecules were destroyed quickly in the spectroscopic measurements that required high molecular densities, they can survive for very long times ($\sim$10 s) in experiments where the excitation is more modest (such as the Surko and Reif experiment [8]). If the excitation density is lower, then one can see contributions from $He_2(a^3\Sigma_u^+)$ decay as well; this was demonstrated in the recent experiments of McKinsey *et al.* using a weak radioactive source drawn quickly out of a liquid-helium bath [26].

Other experiments using weak radioactive sources were carried out by the Hereford group at the University of Virginia in 1970s [6,27–29]. But instead of looking at atomic and molecular spectra, these experiments used a wavelength shifting fluor deposited on the cavity walls to convert the EUV scintillation light to the visible. This had the drawback of not being able to discriminate different atomic and molecular states, but allowed the study of individual decay events. Several interesting results followed from this work. First, it was found that the scintillation pulse height from an α source decreased significantly as the helium was cooled. As mentioned above, this was one of the first pieces of evidence for the creation of metastable excited states in the liquid helium. Second, it was shown that the pulse height could be reduced by the application of an electric field. Third, it was found that the excited liquid helium emits a large number of photons well after the initial scintillation pulse. The rate of delayed photons depended on both temperature and the size of the helium bath, suggesting that the photons were emitted by metastables that diffused through the liquid helium and were quenched when they hit the wall.

Although the Hereford *et al.* experiments were able to detect individual scintillation events and elucidate several important aspects of the helium scintillation process, the time dependence of the helium scintillations was not measured.

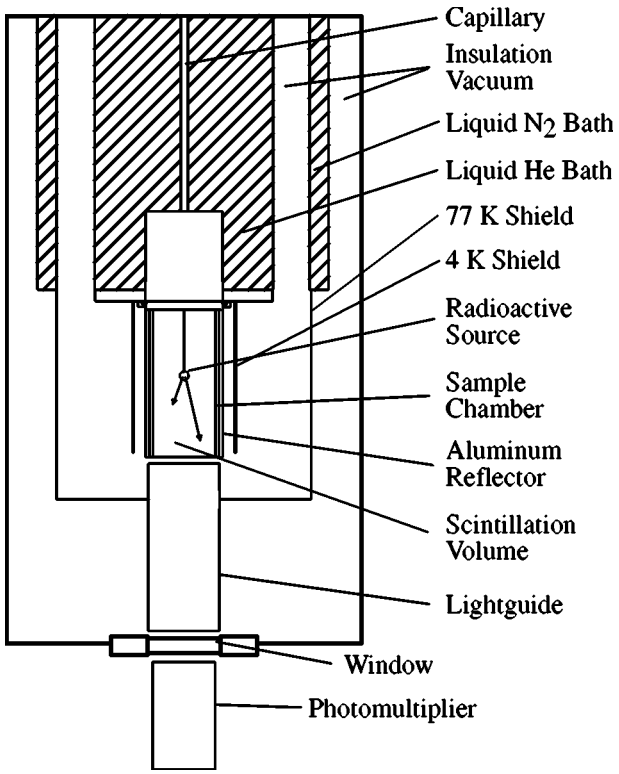

FIG. 1. Apparatus used for initial tests of helium scintillation. The acrylic tube is 30 cm long and 5 cm in diameter, with 3-mm thick walls.

Here we report results on the time dependence of the liquid-helium scintillation signal on the ns to ms time scale. These measurements illuminate the complex dynamics of the scintillation process and its interplay with liquid-helium superfluidity. This work was, in part, motivated by the application of liquid helium as a scintillator. Experiments that do or could make use of helium scintillators are the search for the neutron electric dipole moment [30], the measurement of the neutron β-decay lifetime [31], and the detection of low-energy solar neutrinos [32,33].

II. EXPERIMENTAL APPARATUS

We used several different detection systems, employing different combinations of light collection and fluor geometry to study helium scintillation: (a) a 5-cm diameter acrylic/polystyrene tube at 1.8 K, (b) a 3.9-cm diameter acrylic/polystyrene tube at temperatures down to 250-mK, and (c) a 8.4-cm diameter Gore-tex tube [34]. In every system, a photomultiplier tube was used to detect the fluor emission.

A. Experiments at 1.8 K

Initial experiments were performed with an "a"-type apparatus cooled to 1.8 K through thermal contact with a pumped liquid-helium bath. A schematic of this apparatus is shown in Fig. 1. The sample region was filled with superfluid helium and contained a detector insert with a radioactive source (^{207}Bi or ^{210}Po) held in the center. Alternately, the cell could be exposed to a neutron beam in lieu of a radioactive source. By doping the helium with ^{3}He, the neutron capture events from the reaction $^3\mathrm{He}(n,p)^3\mathrm{H}$ could be observed.

The detector insert is an acrylic tube whose inside surface was coated with tetraphenyl butadiene (TPB)-doped polystyrene. In this approach, the TPB-polystyrene coating converts the EUV scintillation light to blue light. This TPB-polystyrene mixture was tested and found to have good EUV-to-visible conversion properties (fluorescence efficiency of 40%) [35]. Polystyrene doped with TPB is transparent to visible light and can be index matched to light guides, allowing efficient transportation of visible light out of the detection region [36]. The tube is 30 cm long and 5 cm in diameter, with 3-mm thick walls. Some of the blue light created by the conversion of the EUV by the TPB is then trapped in the tube walls, and a fraction of this light makes it to the end of the tube. This light then passes into an acrylic light guide, through a window and a light guide extending from 77 K to 300 K, and then is detected using a photomultiplier tube at room temperature.

The acrylic tubes were coated with TPB-doped polystyrene using the following procedure. First, the acrylic tube was cut to length (30 cm) and its ends polished. Only the ultraviolet transmitting grade (UVT) acrylic was used to maximize the blue light transmission. Then a mixture of research grade toluene, crystalline TPB, and polystyrene was stirred and heated within a beaker. When the mixture was dissolved and warm, the acrylic tube was lowered about 1 cm into the liquid. The top of the tube was connected to a hose that was used to raise the liquid level in the tube by suction. After a few seconds, the liquid level was allowed to slowly drop (over a 20 s period). The tube was then set aside to dry. When dry, the tube was wrapped with an alumnum foil and a TPB-coated acrylic window was epoxied to the bottom of the tube.

The photomultiplier tube used for these measurements was the Burle 8850. This 5-cm diameter tube has a bialkali photocathode and maximum sensitivity at 400 nm, well matched to the emission of TPB. Its high gain also allows clear discrimination of single photoelectron pulses from the noise. The time dependence of the scintillation signal was recorded using a digital oscilloscope.

An average pulse from helium excitation by ^{210}Po, an α emitter, is shown in Fig. 2. This fast pulse is $\approx$10 ns wide and yields about twothirds of the total scintillation signal (the rest coming out on a longer time scale). The time dependence at later times is shown in Fig. 3 and exhibits an exponential decay following the main pulse and a slower decay (proportional to t^{-1}) at later times. This exponential fluorescence decay is different for a cold helium gas sample than for a helium liquid sample; this shows that this decay is not solely a result of a slow decay in the TPB, but rather is indicative of a process in the liquid helium.

B. Experiments between 250 mK and 1.8 K

Later experiments [37] used an apparatus that could be cooled as low as 250 mK, allowing the study of helium scintillations over a wider temperature range. At first, a tube

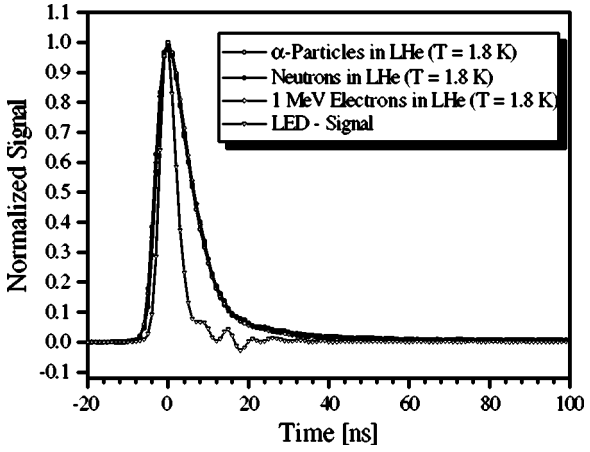

FIG. 2. Averaged pulse observed from helium excitation.

design similar to the one above was used without the end cap and the alumnum foil was replaced with Tyvek paper [38]. Later, a second detector design (see Fig. 4) used two sheets of TPB- coated Gore-tex rolled into tubes and placed end-to-end, making a tube that is 35 cm long and 8.4 cm in diameter. Each sheet is first cut to a rectangle 17.5 cm$\times$28 cm. The sheets are then placed in an organic evaporator and coated with TPB. The density of TPB on the Gore-tex is not uniform and is estimated to be between 200 $\mu g\,cm^{-2}$ and 400 $\mu g\,cm^{-2}$. The TPB absorbs EUV light and fluoresces in the blue, with a peak wavelength of 440 nm. Blue photons, after being emitted by the TPB, on average reflect several times from the TPB coated Gore-tex before escaping out through one of the two tube ends. Some of the blue light is absorbed by the TPB coating, which is not a perfect reflector.

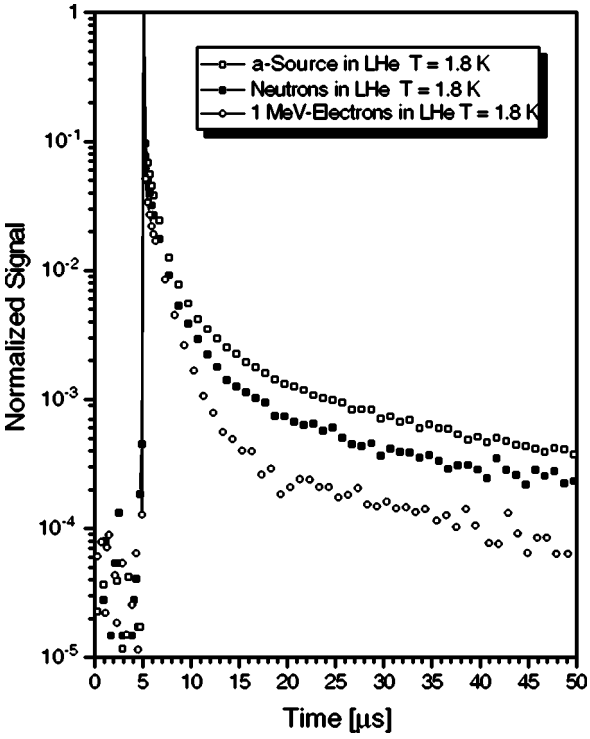

FIG. 3. Average time dependence of PMT voltage signal following excitation of helium by αs, βs, and neutron captures.

Tests in this second apparatus were performed using both α and β sources. The alpha source was ^{210}Po, with an energy release of 5.3 MeV. Also used was ^{113}Sn, a conversion β source with a line energy of 364 keV. In both cases, it is not expected that different ionization tracks interfere significantly in these experiments, since the sources of radiation that we use are relatively weak.

As in the first apparatus, we observe a strong exponential tail following the prompt pulse, with $\approx$1.6 μs lifetime. This tail is present during α, β, or neutron excitation. Experimental traces illustrating this decay is shown in Figs. 5 and 6. These traces were taken by triggering a multichannel scalar (MCS) [39] on the prompt pulses from a ^{113}Sn beta source in a Gore-tex based detector and counting single-photon afterpulses. The average number of photoelectrons in the main pulse was 34.5.

In addition to the 1.6-μs exponential decay, there is a component decaying with a t^{-1} dependence (see Fig. 7). The intensity of this component in β excitation is significantly weaker than in α excitation and neutron capture. For α excitation, the intensity of this component decreases as temperature is lowered from 1.0 K to 0.5 K as shown in Fig. 8. For β excitation, no temperature dependence was observed. No observations of the temperature dependence were made for neutrons. It was verified that the afterpulsing does not originate in the photomultiplier tube by stimulating the photomultiplier tube with an LED to give a pulse size comparable to that made by the helium; in this case no afterpulsing signal was observed.

Since the t^{-1} component is much weaker in β excitation, it could in principle be used to discriminate between electronlike events (e.g., Compton scattering of γ rays) from heavy-ionizing events. This could prove useful in the discrimination of ^{3}He$(n,p)^3$H events from the background γ rays. An analysis of data is shown in Fig. 9, in which the apparatus was exposed to both neutrons and γ rays, showing that the two event populations can be discriminated based on the number of afterpulses. The ratio of short-term pulse height to the number of long-term afterpulses is a good indication of whether the event is a neutron absorption or a γ ray. This type of analysis might also be used for the discrimination of background γ rays from the elastic scattering of weakly interacting massive particles (WIMPs) in a dark matter detector.

III. DISCUSSION

As an ionizing particle passes through liquid helium, it transfers most of its energy to low-energy secondary electrons, which in turn deposit energy in localized spherical regions with high density of excited atoms, free electrons, and ions. The energy deposition per unit length (dE/dx) depends strongly on the charge and mass of the exciting particle. The variation in dE/dx has a big effect on the dynamics of the particles created in the track. In a simplified model, because a high-energy electron deposits on an average 50 eV μm^{-1}, and the energy to ionize a helium atom is 24.6 eV, it follows that ionization events are separated by an average distance of 500 nm. With an average separation of

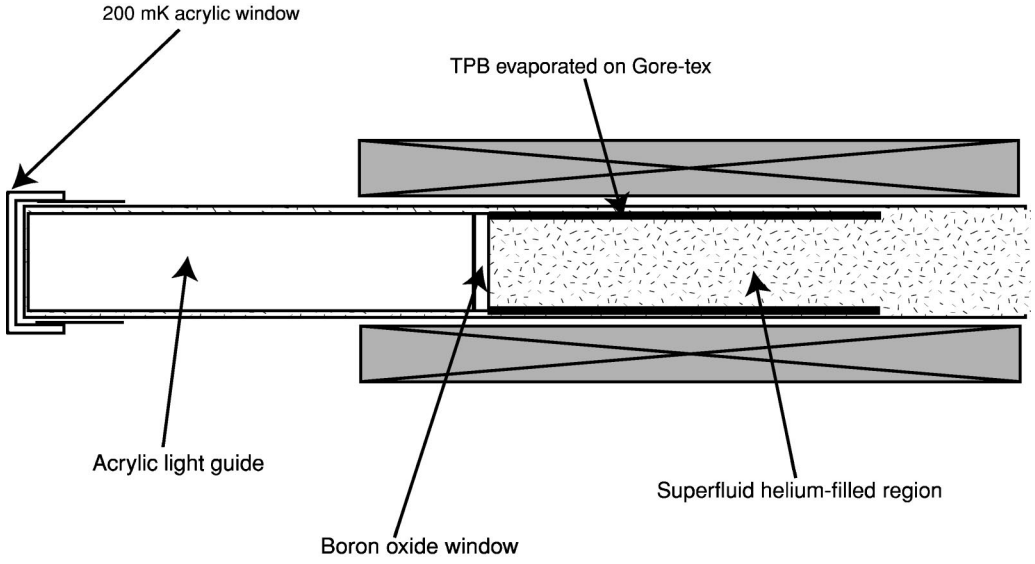

FIG. 4. The Gore-tex tube-based detection cell.

20 nm between the ion and its lost electron, it is clear that ion-electron pairs are well separated under β excitation [40]. However, under α excitation, the energy deposition is 2.5×10^4 eV μm^{-1}, yielding an average spacing between events of only 1 nm, resulting in an overlap between individual ionization events. Although the dynamics of the individual tracks are considerably more complicated, the basic fact is that the energy loss in the case of βs is spread over a much greater volume than that of the αs. Because of the overlap, we expect the α tracks to be cylindrical, while in the case of βs, we would expect the ionization track to consist of separate localized spherical regions [48].

In either case, the excited atoms, electrons, and ions quickly thermalize with the liquid helium. The electron, once thermalized, forms a bubble in the liquid, pushing away the surrounding helium atoms. Experiments on electron bubbles show that the bubble formation happens within 4 ps [41]. The bubble displaces a large number of helium atoms; therefore, the electron has a large effective mass ($\sim$240 helium atoms) and moves slowly through the liquid.

The He^+ ion reacts between 100 ps and 500 ps with the surrounding helium to form He_2^+. It forms in a high vibrational state [42,43], but soon drops to a lower vibrational state through inelastic collisions with surrounding helium atoms. Then, the $He_2{}^+$ ion can react again to form a triatomic ion:

$$He_2{}^+ + He \rightarrow He_3{}^+ .$$

This ion is thought to then form the core of a helium "snowball," which forms within 5 ps [44]. In a snowball, the surrounding helium atoms are attracted to the $He_3{}^+$ ion. The snowball has an effective mass of 40 helium atoms (not as large as the electron bubble).

As mentioned earlier, the average distance between the electron bubble and its parent ion is 20 nm. Based on this initial separation and the effective snowball mass, the average recombination time is 0.3 ns for electron excitation. The ion production and recombination process has been studied carefully by Benderskii *et al.* [45]. A helium snowball will react with a free electron as follows:

$$(He_3^+)_{snowball} + (e^-)_{bubble} \rightarrow He_2 + He.$$

This reaction is the source of large numbers of He_2 molecules, produced in both triplet and singlet states. The singlet states decay immediately, producing a bright pulse of EUV light. This mechanism, presumably, is the source for the 10-ns wide pulse seen in our experiments.

After the prompt pulse, the $He_2(A^1\Sigma_u^+)$ molecules are eliminated, the remaining electronic excitations are then singlet atoms, triplet atoms, and triplet molecules. The interac-

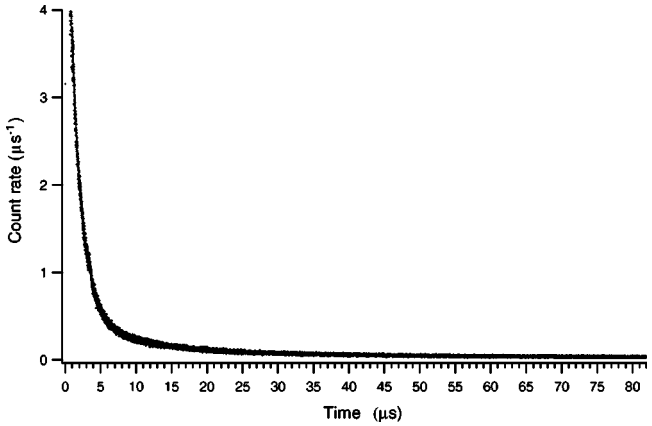

FIG. 5. Afterpulse intensity from a β source, as a function of time, plus a fit to the function $Ae^{-Bt} + Ct^D + E$, where t is measured in milliseconds. The best-fit values are $A = 3.10 \pm 0.03$ μs^{-1}, $B = 0.590 \pm 0.002$ μs^{-1}, $C = 2.06 \pm 0.02$ μs^{-1}, $D = -0.980 \pm 0.004$, and $E = 0.0050 \pm 0.0003$ μs^{-1}. These data were taken at a temperature of 150 mK using a Gore-tex cell. Data were collected in 5 ns bins. There is an average of 34.5 photoelectrons in the main pulse (first 1.0 μs).

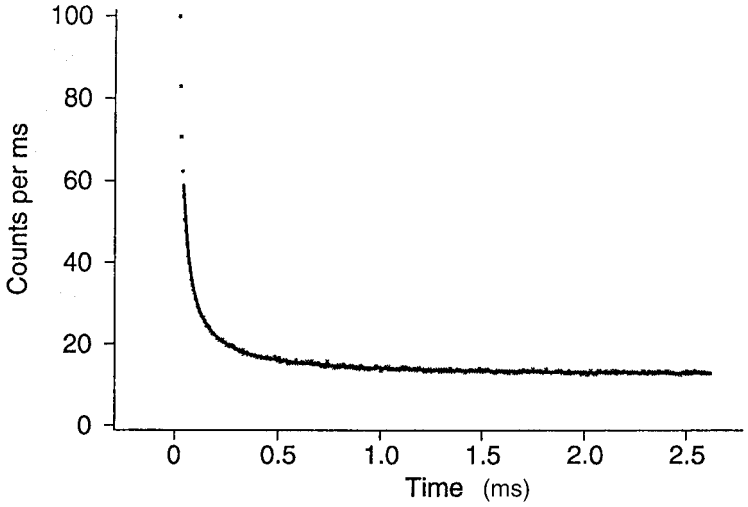

FIG. 6. Afterpulse intensity from a β source, as a function of time, plus a fit to the function At^p+B, where t is measured in μs. For a fit starting at 40 μs, the best-fit values are $A=1.72\pm0.02\ \mu s^{-1}$, $p=-0.976\pm0.003$, and $B=0.01205\pm0.00001\ \mu s^{-1}$. These data were taken at a temperature of 150 mK using a Gore-tex cell. Data were collected in 160 ns bins. There is an average of 34.5 photoelectrons in the main pulse (first 1.0 μs).

tions between these species within the ionizing track can result in more scintillation light following the prompt component. Because the excitation density depends on the kind of ionizing radiation, different ionizing particles can exhibit different afterpulsing time dependence. As the excitation track spreads in size and excitations are removed, the rate of reactions decreases. The time dependence and intensity can therefore depend on the mobility and density of these excitations.

The short-time afterpulsing fits well to a single exponential, with a 1.6-μs decay lifetime. We hypothesize that this scintillation tail derives from a metastable entity reacting with the background helium. A plausible candidate is the metastable atom He(2^1S). There is an evidence from spectroscopic measurements of electron-beam excited liquid helium that this particular atom species reacts with the surrounding helium atoms to form the $He_2(A^1\Sigma_u^+)$ molecule, which then can radiatively decay immediately [20]. Though the time scale of this process has never been measured, a similar reaction with He(2^3S) atoms has been shown to occur with a 15-μs characteristic lifetime [17].

A. Physical models for the t^{-1} component

The source of the t^{-1} component is uncertain, though there are several possible mechanisms. A strong clue is the observation that this component is significantly reduced in β excitation. The main difference between α and β excitation is the density of ionization; β sources in liquid helium will have a path length on the order of 1 cm, while an α will only travel about 2.5×10^{-2} cm [29]. Therefore, it is probable that the mechanism relies on multibody interactions; it does not derive from a species interacting solely with the surrounding ground-state helium, as is the case with the purely exponential decay discussed above. Another clue is that there are not many species that are known to be stable for long times in liquid helium and carry enough energy to make photons: metastable $He_2(a^3\Sigma_u^+)$ molecules, free electrons, and ions. There are then three distinct models that come to mind: $He_2(a^3\Sigma_u^+)$ molecules interacting with each other, $He_2(a^3\Sigma_u^+)$ molecules interacting with ions or electrons, or from the recombination of ions and electrons. Let us examine each of these models in turn.

Metastable-metastable interactions are a well-known phenomenon in organic scintillators [46,47]. In these materials, as in liquid helium, both singlet and triplet states are excited. And as in liquid helium, the singlet states decay rapidly, leaving triplet states still carrying chemical energy from the original ionizing event. Following King and Voltz [48], the concentration of triplet states c_T then evolves as

$$\frac{\partial c_T(r,t)}{\partial t}=D_T\nabla_r^2 c_T(r,t)-\chi_{tt}c_T^2(r,t)-\frac{1}{\tau_T}c_T(r,t),$$

where D_T is the triplet diffusion coefficient, χ_{tt} is the triplet destruction coefficient, and τ_T is the triplet lifetime. In this model, triplet destruction can feed singlet creation. If triplet destruction can create singlets with rate k_{tt}, then light will be produced at a rate proportional to $\chi_{tt}k_{tt}$. In liquid helium,

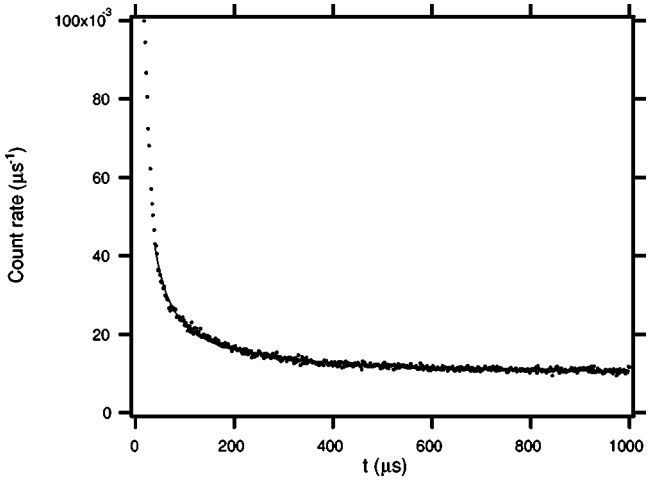

FIG. 7. Afterpulse intensity of an alpha source as a function of time, plus a fit to the function At^p+B, where t is measured in milliseconds. The parameter p fits to -0.987 ± 0.005. These data were taken at a temperature of 1.8 K using an acrylic tube-based cell with 2 μs bins.

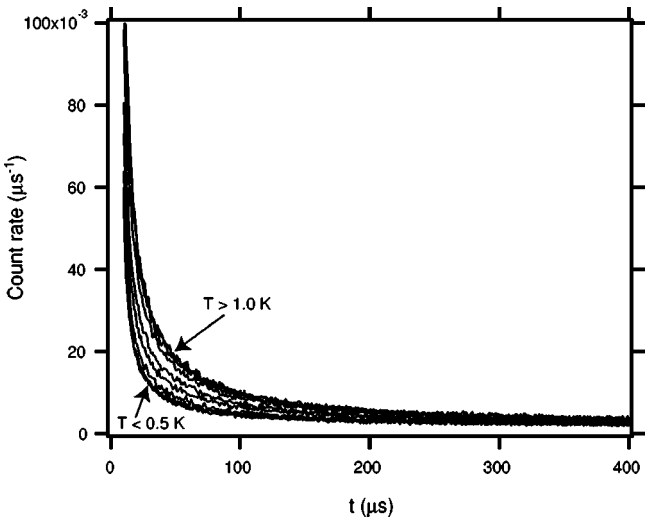

FIG. 8. Afterpulse intensity of an alpha source as a function of time. The curves shown correspond to different helium bath temperatures (220 mK, 360 mK, 500 mK, 670 mK, 780 mK, 830 mK, 880 mK, 960 mK, 1060 mK, and 1140 mK). The intensity of the afterpulsing increases as the temperature is raised from 500 mK to 960 mK.

an appropriate mechanism for triplet-triplet annihilation is Penning ionization, for which the reaction rates have been measured previously [16].

The above equation is nonlinear, and must be solved using approximation methods. The triplet decay term $1/\tau_T c_T(r,t)$ can be ignored, as the triplet lifetime is very long compared to the time scale of the track dynamics. In the case of α excitation, we assume the track to be cylindrically symmetric and Gaussian, i.e., $c_T(r,0)=c_T(0)e^{-(r/r_0)^2}$, where r_0 is the initial width of the track. In the limit that diffusion dominates the triplet annihilation, it's easy to see that the triplet density at the center of the track decreases as $(1+t/t_d)^{-1}$, where $t_d=r_0^2/4D_T$. On the other hand, if triplet annihilation dominates, then the density of triplets would decrease as $(1+t/t_{tt})^{-1}$, where $t_{tt}=1/[\chi_{tt}c_T(0)]$. Depending on whether t_d or t_{tt} is smaller, either diffusion or annihilation controls the process. Under the approximation that the track continues to be Gaussian as the track expands, the rate of singlet radiation from triplet annihilation $I'(t)$ can be shown to be [48]

$$I'(t)=\frac{k_f k_{tt}\tau_s}{2\chi_{tt}t_{tt}}\frac{N_T(0)}{\left[1+\frac{t_d}{2t_{tt}}\ln\left(1+\frac{t}{t_d}\right)\right]^2\left(1+\frac{t}{t_d}\right)},$$

where k_f is the radiative rate parameter for fluorescence emission and $N_T(0)$ is the total number of triplet states formed along one-particle track. For the case of α particles in liquid helium, this expression can be simplified. After the α particle excites the helium, the temperature within the α track rises considerably. If the α particle deposits 5.3 MeV in a volume of 8×10^{-13} cm^3 (for a track of radius 30 nm and length 0.025 cm), then the temperature should rise to about 2 K. At this temperature, D_T should be about 4×10^{-4} cm^2 s^{-1} [29]. Then $t_d=r_0^2/4D_T=25$ ns. The annihilation time $t_{tt}=1/[\chi_{tt}c_T(0)]$ will be much longer, about 125 ns, as χ_{tt} is 2×10^{-10} cm^3 s^{-1} at a temperature of 2.0 K (as measured in electron-bombarded superfluid helium [16]), and the concentration c_T should be about 4×10^{16} (for 30 000 metastables in the track). At later times, the ratio t_d/t_{tt} should decrease further, as D_T will increase somewhat as the temperature within the track drops. In the limit $t_{tt}\gg t_d$ and $t\gg t_d$, the afterpulsing rate varies approximately as t^{-1}.

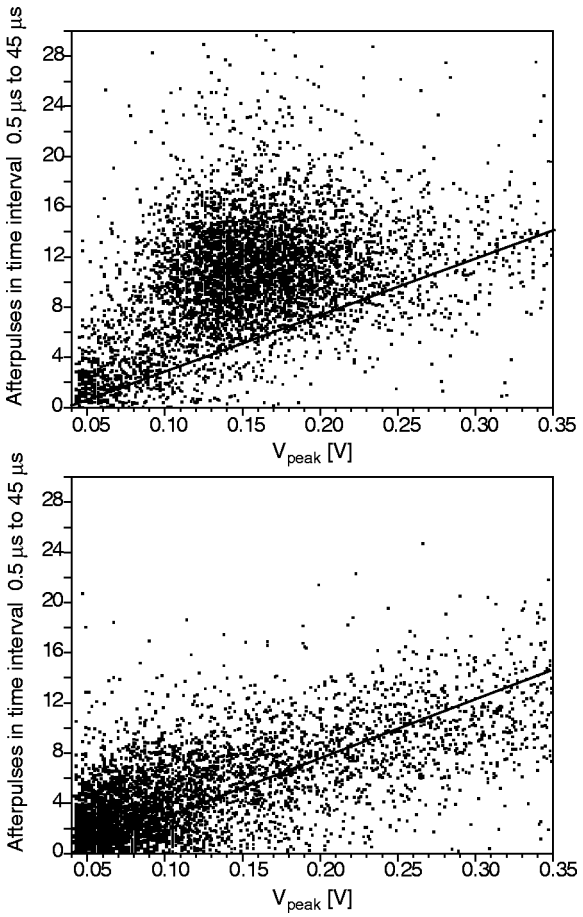

FIG. 9. Scatter plot, in which the 10-ns pulse height is plotted against the number of afterpulses in the time interval of 0.5 μs to 4.5 μs after the prompt pulse. The scatter plot data for a cell exposed to both neutrons and γ rays can be divided into two populations, representative of neutron absorption events and γ ray scattering events. In the first graph, data are shown for a cell with ^{3}He added to the liquid helium. The resulting ^{3}He$(n,p)^3$H events can be distinguished from the γ ray events through their ratio of pulse size to afterpulse number. In the second graph are shown data for a cell without ^{3}He added.

Because the initial temperature of the helium within the track is predominantly determined by the energy deposition by the α particle, the intensity of the t^{-1} afterpulsing component has weaker dependence on the temperature of the helium bath than the diffusion coefficient does. The observed temperature dependence can be explained by a lower density of metastable molecules at lower temperatures, which can in

turn be attributed to a more rapid radial spreading of the ionization track immediately following the initial event. Roberts and Hereford have shown that the temperature dependence of the prompt pulse size from αs in liquid helium can be explained by this hypothesis; they observe this effect as the temperature is dropped from 1.2 K to 0.6 K [29]. The similarity of this temperature range to the temperature range in which the afterpulsing varies in intensity indicates that the two phenomena are closely linked, and indeed may be identical. The fact that the afterpulsing does not continue to decrease as the temperature is lowered below 0.5 K must then indicate that the expansion of the track below 0.5 K is not inhibited by scattering from excitations in the surrounding liquid helium, but instead is limited by scattering among its own constituents.

For β excitations, one expects the ionizations to be localized in isolated spherical regions. In this case, a similar analysis predicts a $t^{-3/2}$ dependence that is not observed in our data; the βs instead show a t^{-1} dependence. This coupled with the temperature independence of the β afterpulsings means that King and Voltz model does not fit well to the observations in βs. However, as the above-mentioned track heating is much less significant for the βs (t_d will be much less) and the fact that the t^{-1} afterpulsing due to the βs is temperature independent suggests that the β track expansion might be limited by similar effects that limit the α expansion at low temperatures. Further, because the mean-free path of βs is much longer, the initial spherical regions could undergo rapid expansion before diffusion kicks in. The spherical regions essentially merge into a cylindrical geometry after the expansion and it follows that the afterpulsing signal should then go as t^{-1} as we observed.

A second explanation for the afterpulsing is metastable destruction from scattering with some other, more stable species. These more stable species would probably be helium ions or electrons, as there are no other candidates that would last for the long times required. This explanation is favored by Roberts and Hereford in their model for α- particle prompt scintillation; they claim that the temperature dependence they observe is not fit well by metastable-metastable annihilation [29]. However, their model for the metastable-stable species interaction is equivalent to $(1+t/a)^{-b}$, where both a and b are inversely proportional to the diffusion coefficient and thus strongly temperature dependent. Their model also does not take the α track heating into account. Our observation of the t^{-1} time dependence contradicts this model.

Even if we take the track heating into account, it seems highly unlikely that many electrons escape quick recombination; it is estimated that the average recombination time is 0.3 ns [40]. In the Onsager theory, the probability of an electron-ion pair losing each other is proportional to e^{-r/r_0}, where $r_0=\epsilon e^2/kT$, and ϵ is the dielectric constant. Therefore, r_0 increases greatly at lower temperatures, and it is quite unlikely for an electron and ion in liquid helium to escape prompt recombination.

The third explanation for the afterpulsing is ion-electron recombination. In this model, a fraction of the electrons and ions released as a result of the α particle do not recombine immediately, but escape to a large enough distance from each other that they are not attracted significantly by each other's field. Instead, they find each other on microsecond time scales, recombining to form singlet molecules that immediately decay. Again, a t^{-1} dependence is possible if diffusion is the dominant process determining the density of the interacting species. Kane *et al.* used this model to explain their observation of the pulse height versus temperature for α and β excitations [5]. The fact that the α pulse height showed a strong temperature dependence below the λ point while the β pulse height was independent of the temperature was attributed to the recombination of the electron-ion pairs being modulated by the mobilities in the case of the dense α track. For the widely separated beta track, recombination is expected to play a less significant role. If, on the other hand, recombination dominates over diffusion, then the reaction should proceed as t^{-2}, as the density of electrons and ions each varying as t^{-1}. Experiments measuring scintillation in liquid xenon do see an afterpulsing tail attributable to recombination, and it decays as t^{-2}. In similar experiments in liquid krypton and liquid argon, a recombination tail is not seen; this is attributable to a recombination cross section that increases for the lighter noble gases, and the lower temperatures of their liquids [49]. In the xenon experiments, the tail could be eliminated through the application of an electric field [49]. Similarly, this explanation for the afterpulsing in liquid helium could be tested by the application of an electric field. Again, it seems unlikely that many electrons escape recombination in the case of αs, because of the low temperature of the helium and small average distance between electron and parent ion.

Thus, it would seem that either metastable-metastable destruction, metastable-stable destruction, ion-electron recombination, or some combination of the three could be the source of the t^{-1} afterpulsing component. Each of these solutions assumes that the species responsible for the afterpulsing diffuses outward from the ionization track. Metastable-metastable interactions seem to be the most plausible scenario, as electron-ion recombination in liquid helium is known to be quite efficient and because recombination should be enhanced at liquid-helium temperatures. On the other hand, helium is unique among the noble gases for the extremely long lifetime of its $He_2(a^3\Sigma_u^+)$ molecule, and the fact that liquid helium is also unique in its exhibition of a t^{-1} afterpulsing tail probably reflects this attribute. Further discrimination between these possible solutions might be achieved by the application of an electric field to the excitation region. There seems to be no clear explanation for the β data, further investigation is warranted.

Following the t^{-1} component, no further decay is visible on millisecond time scales. However, there is a large rate of single-photon events, probably related to $He_2(a^3\Sigma_u^+)$ decay. In a previous publication, we reported that removing a radioactive source from liquid helium caused this single-photoelectron rate to decrease exponentially with time. This exponential decay is presumably caused by the radiative decay of $He_2(a^3\Sigma_u^+)$ molecules [26].

IV. CONCLUSION

The time dependence of scintillations in liquid helium have been investigated. It was found that the initial pulse of scintillation light, believed to arise from the radiative dissociation of singlet helium excimers, is approximately 10 ns in length. Later scintillation components include a 1.6-μs component and a t^{-1} component.

In summary, following an ionizing radiation event in liquid helium, the following processes occur

(i) Ionizing radiation passing through liquid helium creates large numbers of excited atoms and molecules.

(ii) The excited atoms and molecules are quickly quenched to their lowest-energy singlet and triplet electronic states, yielding a population of $He_2(A^1\Sigma_u^+)$ and $He_2(a^3\Sigma_u^+)$ molecules and $He(2^1S)$ and $He(2^3S)$ atoms.

(iii) The singlet $He_2(A^1\Sigma_u^+)$ molecules radiatively decay within 10 ns of the original event, releasing an intense pulse of EUV light.

(iv) The excited atoms $He(2^1S)$ and $He(2^3S)$ react with the ground-state helium atoms of the liquid, forming vibrationally excited $He_2(A^1\Sigma_u^+)$ and $He_2(a^3\Sigma_u^+)$ molecules. The $He(2^1S)$ quenching reaction is apparently evident in the afterpulsing data, producing scintillation light on a 1.6 μs time scale.

(v) Triplet $He_2(a^3\Sigma_u^+)$ molecules diffuse out of the ionization track, reacting with each other via the Penning ionization, forming some products that immediately decay, emitting more EUV light. This reaction appears to be especially evident when an α source is used, since the high excitation density in turn yields a high metastable density. The scintillation light created decays inversely with time.

(vi) Triplet $He_2(a^3\Sigma_u^+)$ molecules that make it out of the track diffuse through the liquid helium. Eventually, these molecules either radiatively decay or are quenched at the container walls. The lifetime of these molecules in liquid helium is (13 ± 2) s [26].

ACKNOWLEDGMENTS

We thank Dr. James Butterworth for his contribution to the experimental apparatus. Neutron facilities used in this work were provided by the Hahn-Meitner Institut, Germany, and National Institute of Standards and Technology, MD. This experiment was supported in part by the National Science Foundation under Grant No. PHY-0099400.

[1] E.H. Thorndike and W.J. Shlaer, Rev. Sci. Instrum. **30**, 838 (1959).
[2] H. Fleishman *et al.*, Rev. Sci. Instrum. **30**, 1130 (1959).
[3] J.E. Simmons and R.T. Siegel, Rev. Sci. Instrum. **32**, 1173 (1961).
[4] F.E. Moss and F.L. Hereford, Phys. Rev. Lett. **11**, 63 (1963).
[5] J.R. Kane, R.T. Siegel, and A. Suzuki, Phys. Lett. **6**, 256 (1963).
[6] F.L. Hereford and F.E. Moss, Phys. Rev. **141**, 204 (1966).
[7] J. Jortner *et al.*, Phys. Rev. Lett. **12**, 415 (1964).
[8] C. Surko and F. Reif, Phys. Rev. **175**, 229 (1968).
[9] G.W. Rayfield, Phys. Rev. Lett. **23**, 687 (1969).
[10] R.P. Mitchell and G.W. Rayfield, Phys. Lett. A **37**, 231 (1972).
[11] W.S. Dennis *et al.*, Phys. Rev. Lett. **23**, 1083 (1969).
[12] P. Hill, Phys. Rev. A **40**, 5006 (1989).
[13] A.V. Konovalov and G.V. Shlyapnikov, Sov. Phys. JETP **73**, 286 (1991).
[14] C.O. Chablowski *et al.*, J. Chem. Phys. **90**, 2504 (1989).
[15] J.W. Keto, M. Stockton, and W.A. Fitzsimmons, Phys. Rev. Lett. **28**, 792 (1972).
[16] J.W. Keto, F.J. Soley, M. Stockton, and W.A. Fitzsimmons, Phys. Rev. A **10**, 887 (1974).
[17] J.W. Keto, F.J. Soley, M. Stockton, and W.A. Fitzsimmons, Phys. Rev. A **10**, 872 (1974).
[18] J.R. Woodworth and H.W. Moos, Phys. Rev. A **12**, 2455 (1975).
[19] A. Koymen *et al.*, Chem. Phys. Lett. **168**, 405 (1990).
[20] M. Stockton *et al.*, Phys. Rev. A **5**, 372 (1972).
[21] C.M. Surko, R.E. Packard, G.J. Dick, and F. Reif, Phys. Rev. Lett. **24**, 657 (1970).
[22] M. Stockton, J.W. Keto, and W.A. Fitzsimmons, Phys. Rev. Lett. **24**, 654 (1970).
[23] J.S. Adams *et al.*, J. Low Temp. Phys. **113**, 1121 (1998).
[24] G. W. Seidel, (private communication).
[25] V.B. Eltsov *et al.*, J. Low Temp. Phys. **113**, 525 (1998).
[26] D.N. McKinsey *et al.*, Phys. Rev. A **59**, 200 (1999).
[27] M.R. Fischbach, H.A. Roberts, and F.L. Hereford, Phys. Rev. Lett. **23**, 462 (1969).
[28] H.A. Roberts and F.L. Hereford, Phys. Lett. **38A**, 395 (1972).
[29] H.A. Roberts and F.L. Hereford, Phys. Rev. A **7**, 284 (1973).
[30] R. Golub and S.K. Lamoreaux, Phys. Rep. **237**, 1 (1994).
[31] J.M. Doyle and S.K. Lamoreaux, Europhys. Lett. **26**, 253 (1994).
[32] S.R. Bandler *et al.*, J. Low Temp. Phys. **93**, 785 (1993).
[33] D.N. McKinsey and J.M. Doyle, J. Low Temp. Phys. **118**, 153 (2000).
[34] Unembossed Gore-tex GR gasket material, Gore Corporation (www.gorefabrics.com). Certain trade names and company products are mentioned in the text or identified in illustrations in order to adequately specify the experimental procedure and equipment used. In no case does such identification imply recommendation of endorsement by the National Institute of Standards and Technology, nor does it imply that the products are necessarily the best available for the purpose.
[35] D.N. McKinsey *et al.*, Nucl. Instrum. Methods Phys. Res. B **132**, 351 (1997).
[36] K. Habicht, Ph.D. thesis, Technical University of Berlin, 1998.
[37] D. N. McKinsey, Ph. D. thesis, Harvard University, 2002.
[38] Tyvek spun olefin paper, DuPont Chemical Corporation.
[39] SRS model SR430, Stanford Research Systems, Sunnyvale, CA.
[40] A.G. Tenner, Nucl. Instrum. Methods **22**, 1 (1963).
[41] J.P. Hernandez and M.J. Silver, Phys. Rev. A **2**, 1949 (1970).
[42] B.E. Callicoatt *et al.*, J. Chem. Phys. **108**, 9371 (1998).

[43] B.E. Callicoatt *et al.*, J. Chem. Phys. **105**, 7872 (1996).
[44] M. Ovchinnokov *et al.*, J. Chem. Phys. **108**, 9351 (1998).
[45] A.V. Benderskii *et al.*, J. Chem. Phys. **110**, 1542 (1999).
[46] L.M. Bollinger and G.E. Thomas, Rev. Sci. Instrum. **32**, 1044 (1961).
[47] G. Walter and A. Coche, Nucl. Instrum. Methods **23**, 147 (1963).
[48] T.A. King and R. Voltz, Proc. R. Soc. London, Ser. A **289**, 424 (1966).
[49] S. Kubota *et al.*, Phys. Rev. B **20**, 3486 (1979).